Indian Institute of Technology Delhi

Numerical Simulation of Diffusion Reaction in Porous Catalyst Pellets

Author: **Dhruvraj Gohil**
Department: Chemical Engineering

Abstract

Porous Catalyst pellets are majorly used in chemical industries to increase reaction rates by providing a large surface area. Chemical reactions occur inside porous structures. The rate of the overall reaction and process is limited by how diffusion and reaction interact within the catalyst structure. In this paper we do numerical analysis of diffusion–reaction phenomena in porous spherical catalyst pellets. By solving the reaction-diffusion equations with help of finite difference methods (FDM), Central Difference discretization, Thomas algorithm to get concentration distributions and effectiveness factors. We analyzed non-dimensionalized concentration profiles at different time points for various values using a CPP algorithm. By This analysis we can study the effect of pellet size, diffusivity, and reaction kinetics on catalyst performance, and we can optimize the catalytic reactor design in industry.

Contents

1 Introduction

A catalyst is substance that alter the rate of chemical reaction and which itself is not being consumed in that chemical reaction. It works by providing a different reaction pathway with lower activation energy so it allows reactants to convert into products more efficiently and easily. The porous catalysts are used to increase catalytic performance In many industrial reaction and chemical processes like petroleum refining, environmental catalysis, and chemical manufacturing by providing high surface area with efficient catalytic activity.[3] A porous catalyst contain a network of tiny interconnected pores which provides a large internal surface area where reactions can be done And because of catalyst's porous structure the reactant molecules can move into the catalyst pellet and reach the active sites that are spread across the inner surfaces. When the rate of diffusion is lower than that of the chemical reaction, concentration gradients occur inside the pellet. This results in a decreased in overall rate of reaction compared to the case where the pellet is completely exposed to the bulk concentration. This phenomenon is measured by the effectiveness factor (η) which defined as the ratio of the actual reaction rate within the pellet to the rate that would occur if the entire pellet were at the external (bulk) concentration. The effectiveness of catalysis is highly dependent on the concentration distribution within the catalyst pellet, and the concentration is also varying with the time. so basically, we have a Partial differential equation with derivatives with respect to r and t. And after observing the form of the equation, it was found to be a parabolic PDE, which we tried to solve using computational techniques like FDM, Thomas algorithm, etc.

Analytical solutions for the effectiveness factor are available only for simple geometries such as spherical geometry and for first-order reaction kinetics. In practical catalytic systems reactions are often nonlinear with complex diffusion processes and it makes analytical approaches insufficient. numerical methods are help in interplay between reaction and diffusion in porous catalysts that also provide accurate prediction of spatial concentration distributions and local reaction rates within the pellet.

Effectiveness factor and concentration distributions provides understanding of how reaction order, pellet size, and diffusivity affect catalyst performance.

2 Problem formulation

Problem Explanation:

The reactant moves through the internal pore spaces of a porous catalyst pellet and reacts on the inner active surfaces. As the reactant travels from the outer surface toward the centre, it is gradually consumed by the chemical reaction occurring inside. The combined influence of diffusion and reaction determines how much of the pellet actually participates in the process, which is the basis for calculating the effectiveness factor. The concentration inside the pellet changes depending on how easily the reactant can move through the pores and how fast the reaction takes place at each location. With the help of the concentration profile within the pellet and the overall reaction effectiveness, we can evaluate how the catalyst performs under different reaction and mass-transfer conditions.

Assumptions:

- The catalyst pellet is spherical.
- The system is isothermal.
- Diffusion occurs only within the pores, with constant effective diffusivity
- The reaction is uniform throughout the pellet and depends only on the local concentration.
- Radial symmetry is assumed, with no flux at the centre ($dC/dr = 0$) and surface concentration equal to bulk ($C = C_s$).

3 Numerical approach

3.1 Governing Equation in Spherical Coordinates

The transient mass balance for a reacting species inside a porous spherical pellet is[1]

$$\varepsilon \frac{\partial C}{\partial t} = D_e \left(\frac{\partial^2 C}{\partial r^2} + \frac{2}{r} \frac{\partial C}{\partial r} \right) - R_r(C) \tag{1}$$

where:

- $C(r,t)$: pore-phase concentration ($\mathrm{mol/m^3}$)
- ε: pellet porosity
- D_e: effective diffusivity ($\mathrm{m^2/s}$)
- $R_r(C)$: reaction rate per volume ($\mathrm{mol/m^3/s}$)
- r: radial coordinate (m)

3.1.1 First-Order Reaction

For a first-order reaction:

$$R_r(C) = kC \tag{2}$$

Thus the PDE becomes:

$$\boxed{\varepsilon \frac{\partial C}{\partial t} = D_e \left(\frac{\partial^2 C}{\partial r^2} + \frac{2}{r} \frac{\partial C}{\partial r} \right) - kC} \tag{3}$$

This is a diffusion–reaction PDE in spherical coordinates.

3.2 Boundary Conditions

3.2.1 Initial Condition

$$C(r,0) = 0 \tag{4}$$

3.2.2 Center Symmetry ($r = 0$)

$$\left. \frac{\partial C}{\partial r} \right|_{r=0} = 0 \tag{5}$$

3.2.3 Surface Condition (Dirichlet BC)

$$C(R,t) = C_s \tag{6}$$

3.3 Characteristic Time Scales

- Diffusion time: $t_D = \dfrac{R^2}{D_e}$
- Reaction time: $t_R = \dfrac{1}{k}$

The Thiele modulus:

$$\phi = R\sqrt{\frac{k}{D_e}} \tag{7}$$

3.4 Finite Difference Discretization

[2][5]A uniform radial grid:

$$r_i = i\Delta r, \quad i = 0, 1, \ldots, N \tag{8}$$

$$\Delta r = \frac{R}{N} \tag{9}$$

Discrete concentration:

$$C_i^n \approx C(r_i, t^n) \tag{10}$$

3.4.1 Second Derivative

$$\left.\frac{\partial^2 C}{\partial r^2}\right|_i \approx \frac{C_{i+1}^n - 2C_i^n + C_{i-1}^n}{\Delta r^2} \tag{11}$$

3.4.2 First Derivative

$$\left.\frac{\partial C}{\partial r}\right|_i \approx \frac{C_{i+1}^n - C_{i-1}^n}{2\Delta r} \tag{12}$$

Thus:

$$\frac{\partial^2 C}{\partial r^2} + \frac{2}{r_i}\frac{\partial C}{\partial r} \approx \frac{C_{i+1} - 2C_i + C_{i-1}}{\Delta r^2} + \frac{C_{i+1} - C_{i-1}}{r_i \Delta r} \tag{13}$$

3.4.3 Center Node ($r = 0$)

Symmetry condition:

$$\frac{\partial C}{\partial r}(0, t) = 0 \;\Rightarrow\; C_{-1} = C_1$$

Second derivative at center:

$$\left.\frac{\partial^2 C}{\partial r^2}\right|_0 \approx 2\,\frac{C_1 - C_0}{\Delta r^2} \tag{14}$$

Center node equation:

$$\varepsilon\frac{dC_0}{dt} = 2D_e\frac{C_1 - C_0}{\Delta r^2} - kC_0 \tag{15}$$

3.5 Backward Euler Time Discretization

$$\frac{C_i^{n+1} - C_i^n}{\Delta t} \tag{16}$$

[4]Implicit form:

$$\boxed{\varepsilon \frac{C_i^{n+1} - C_i^n}{\Delta t} = D_e \left(\frac{C_{i+1}^{n+1} - 2C_i^{n+1} + C_{i-1}^{n+1}}{\Delta r^2} + \frac{C_{i+1}^{n+1} - C_{i-1}^{n+1}}{r_i \Delta r} \right) - k C_i^{n+1}} \tag{17}$$

This forms a tridiagonal system.

3.6 Tridiagonal System

$$A_i C_{i-1}^{n+1} + B_i C_i^{n+1} + C_i C_{i+1}^{n+1} = D_i \tag{18}$$

Coefficients:

$$A_i = -D_e \left(\frac{1}{\Delta r^2} + \frac{1}{r_i \Delta r} \right) \tag{19}$$

$$B_i = \frac{\varepsilon}{\Delta t} + \frac{2D_e}{\Delta r^2} + k \tag{20}$$

$$C_i = -D_e \left(\frac{1}{\Delta r^2} - \frac{1}{r_i \Delta r} \right) \tag{21}$$

$$D_i = \frac{\varepsilon C_i^n}{\Delta t} \tag{22}$$

Boundary:

$$C_N^{n+1} = C_s \tag{23}$$

3.7 Thomas Algorithm

General tridiagonal form:

$$a_i x_{i-1} + b_i x_i + c_i x_{i+1} = d_i$$

Forward elimination:

$$m_i = \frac{a_i}{b_{i-1}}, \qquad b_i \leftarrow b_i - m_i c_{i-1}, \qquad d_i \leftarrow d_i - m_i d_{i-1}$$

Back substitution:

$$x_N = \frac{d_N}{b_N}$$

$$x_i = \frac{d_i - c_i x_{i+1}}{b_i}, \qquad i = N-1, \ldots, 0$$

3.8 Effectiveness Factor

The actual reaction rate inside the pellet is:

$$R_{\text{act}}(t) = \int_0^R k\, C(r,t)\, 4\pi r^2\, dr \tag{24}$$

Define:

$$f(r) = k\, C(r,t)\, 4\pi r^2 \tag{25}$$

Using the Simpson 3/8 integration rule:

$$I_h = \int_0^R f(r)\, dr$$

with step size $h = \frac{R}{n}$, where n is a multiple of 3:

$$I_h = \frac{3h}{8}\left[f_0 + f_n + 3 \sum_{\substack{i=1 \\ i \bmod 3 \neq 0}}^{n-1} f_i + 2 \sum_{\substack{i=3 \\ i \bmod 3 = 0}}^{n-3} f_i \right] \tag{26}$$

Half-step integration $I_{h/2}$:

$$I_{h/2} = \text{same formula but using twice as many points}$$

Richardson extrapolation for error reduction:

$$R_{\text{act}} \approx I_{\text{rich}} = \frac{16\, I_{h/2} - I_h}{15} \tag{27}$$

The ideal rate (no diffusion resistance) is:

$$R_{\text{ideal}} = k\, C_s \left(\frac{4}{3} \pi R^3 \right) \tag{28}$$

The effectiveness factor is:

$$\eta = \frac{I_{\text{rich}}}{R_{\text{ideal}}} \tag{29}$$

4 Observation

4.1 Graphs

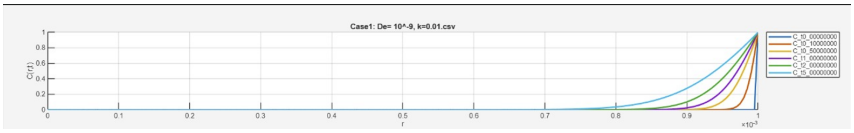

Figure 1: Transient concentration profiles for $D_e = 1 \times 10^{-9}\,\mathrm{m^2/s}$, $k = 0.01\,\mathrm{s^{-1}}$ (weak diffusion limitation).

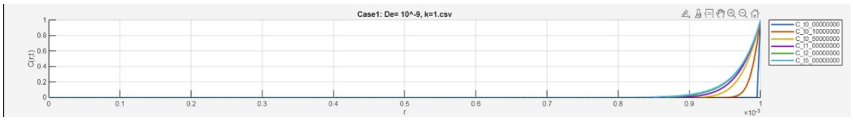

Figure 2: Transient concentration profiles for $D_e = 1 \times 10^{-9}\,\mathrm{m^2/s}$, $k = 1\,\mathrm{s^{-1}}$ (strongly diffusion-limited).

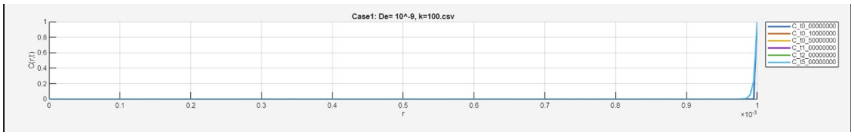

Figure 3: Transient concentration profiles for $D_e = 1 \times 10^{-9}\,\mathrm{m^2/s}$, $k = 100\,\mathrm{s^{-1}}$ (extreme diffusion limitation).

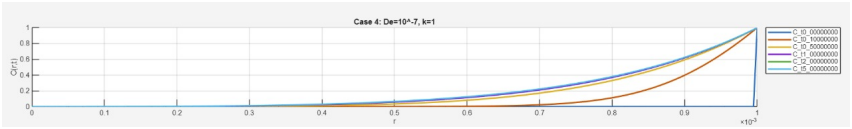

Figure 4: Transient concentration profiles for $D_e = 1 \times 10^{-7}\,\mathrm{m^2/s}$, $k = 1\,\mathrm{s^{-1}}$ (balanced diffusion–reaction).

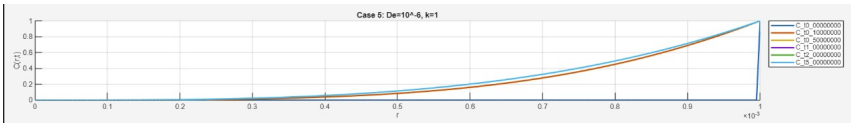

Figure 5: Transient concentration profiles for $D_e = 1 \times 10^{-6}\,\mathrm{m^2/s}$, $k = 1\,\mathrm{s^{-1}}$ ($\phi \approx 1$, balanced control).

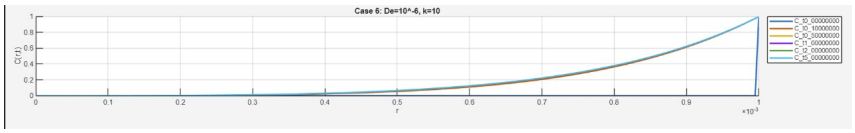

Figure 6: Transient concentration profiles for $D_e = 1 \times 10^{-6}\,\mathrm{m^2/s}$, $k = 10\,\mathrm{s^{-1}}$ (moderately diffusion-limited).

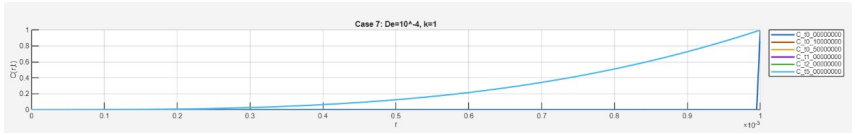

Figure 7: Transient concentration profiles for $D_e = 1 \times 10^{-4}\,\mathrm{m^2/s}$, $k = 1\,\mathrm{s^{-1}}$ (reaction-limited; nearly uniform concentration).

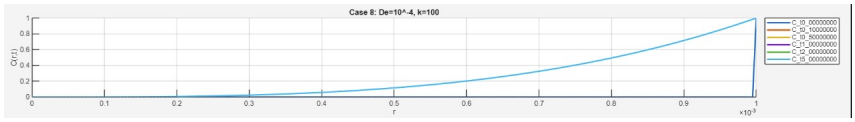

Figure 8: Transient concentration profiles for $D_e = 1 \times 10^{-4}\,\mathrm{m^2/s}$, $k = 100\,\mathrm{s^{-1}}$ (mixed regime, $\phi \approx 1$).

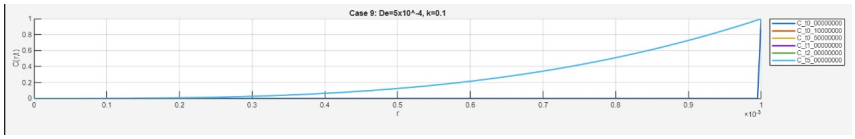

Figure 9: Transient concentration profiles for $D_e = 5 \times 10^{-4}\,\mathrm{m^2/s}$, $k = 0.1\,\mathrm{s^{-1}}$ (strongly reaction-limited).

4.2 Table

Diffusion–Reaction Regime Classification

Case	De (m2/s)	k (1/s)	tD (s)	phi	Regime Description
1	1e-9	0.01	1000	3.1623	Weak diffusion limitation, mixed regime
2	1e-9	1	1000	31.6228	Strongly diffusion limited
3	1e-9	100	1000	316.2278	Extremely diffusion limited; thin reacting zone
4	1e-7	1	10	3.1623	Balanced diffusion reaction
5	1e-6	1	1	1.0000	Balanced control; transient penetration around tD
6	1e-6	10	1	3.1623	Moderately diffusion limited
7	1e-4	1	0.01	0.1000	Reaction limited; uniform concentration
8	1e-4	100	0.01	1.0000	Mixed regime
9	5e-4	0.1	0.002	0.014142	Strongly reaction limited

Table 1: **Effectiveness for $D_e = 10^{-6}$ and $k = 1$**

Time	Effectiveness Factor
0.000000	0.007174
0.010000	0.223263
0.500000	0.488001
1.000000	0.488014
1.500000	0.488014
2.000000	0.488014
2.500000	0.488014
3.000000	0.488014
3.500000	0.488014
4.000000	0.488014
4.500000	0.488014
5.000000	0.488014

5 Results and Discussion

The transient concentration profiles inside the spherical catalyst pellet depend on the relative magnitude of time with respect to the diffusion time scale, $t_D = R^2/D_e$. Initially, when $t < t_D$, reactant penetrates only till a thin layer near the pellet surface. Significant internal concentration gradients appear, and the concentration inside remains zero, which tells us about limitations in diffusion and catalytic reaction in the pellet. As time approaches the diffusion time scale, $t \approx t_D$, the diffusion front moves deeper, and concentration gradients begin to flatten. Both diffusion and catalytic reaction change the concentration of the pellet, and the pellet core also becomes active here. When $t > t_D$, the pellet reaches its saturation level, and the concentration profile becomes uniform throughout the radius. Diffusion effectively overcomes the internal resistance, allowing the reactant to reach all active sites. As a result, the pellet approaches a quasi-steady, fully developed concentration distribution.

Through time scale we can analyse the noticeable effect of effective diffusivity D_e on concentration. When D_e is low, reactant penetration is slow and diffusion resistance dominates. Even later, the pellet shows steep internal gradients, with the central region unreacted. This limitation of diffusion leads to restricted effective use of catalyst which leads to low effectiveness. When the diffusivity is high, diffusion time becomes very small leading to rapid movement of reactant inside the pellet. This results in uniform concentration profiles and minimal internal resistance. The entire pellet volume is now available for reaction early, which results in the effectiveness factor reaching unity. These results confirm that diffusivity plays a role in determining the extent of internal mass transfer limitations.

The way effectiveness factor changes over time shows how the concentration inside the pellet changes. Initially, the effectiveness factor is almost zero because only a very thin outer layer of the pellet is exposed to reactant. As diffusion occurs and more internal regions get involved, the effectiveness factor increases sharply,

indicating a rise in overall reaction rate. When the pellet reaches saturation, the effectiveness factor converges to its steady-state value, exactly like predictions for spherical pellets in first-order kinetics. This time dependency confirms the accuracy of the numerical method and illustrates the physical connection between diffusion penetration and catalytic activity.

The reaction rate constant k plays a role in influencing the internal behaviour of the catalytic pellet. For small k, reaction is slow as compared to diffusion, and concentration remains uniform in the pellet, which results in high catalyst use and an effectiveness factor close to unity, indicating minimal mass transfer resistance. When k is moderate, internal concentration gradients increase, which indicates a balance between reaction and diffusion. There are little limitations in diffusion and the effectiveness factor is somewhere in between, neither too low nor too high. For large k, the reaction is very fast relative to diffusion, which causes immediate consumption of reactant near the surface. As a result, steep gradients develop, the pellet centre remains unreacted, and only a thin outer region participates in the reaction. In this case, the effectiveness factor becomes very low, showing the inability of diffusion to keep up with the reaction rate. These statements align with classical Thiele modulus theory.

The combined analysis of diffusivity D_e and reaction rate constant k demonstrates that the balance between diffusion and reaction is managed by their ratio, represented by the Thiele modulus $\phi = R\sqrt{k/D_e}$. High diffusivity and low reaction rate (small ϕ) lead to uniform concentration profiles and high effectiveness factors, representing controlled reaction operation. Low diffusivity with high reaction rate (large ϕ) produces steep concentration gradients and low catalyst use, indicating a strongly diffusion-limited system. Intermediate values of both parameters generate mixed control behaviour where neither mechanism dominates fully. Overall, the numerical results capture the entire spectrum from fully reaction-controlled to fully diffusion-controlled systems, showing the strength of the model and highlighting the importance of transport–kinetic interactions in porous catalysts.

6 Conclusions

6.1 Primary conclusions

The work that we have done was able to re-iterate the capability of numerical finite difference methods paired with Euler implicit methods and Thomas algorithm. Using these numerical methods we were able to successfully demonstrate concentration distribution in a spherical catalyst distributed with different time points.[6]

6.2 Analysis of the methodologies

Our major goals while conducting this study was to understand the dependance of profiles with various set parameters. We could successfully re-produce the results given by classical catalysis theory. we could comprehend that at early times when $t < tD(tD = R^2/De)$, the concentration was nearly vanishing towards the inside and after tD the catalyst attains nearly uniform concentration of the reactant.
The effectiveness factor is another important parameter regarding the catalytic properties. When we calculated the effectiveness factor for various Thiele moduls values, It was found out that in the reaction limited regime(lower k vales), the effectiveness factor is very high and in the diffusion limited regime(lower De values), the effectiveness factor was relatively less in magnitude. Steep concentration gradients with r was observed when effectiveness factor reained low, showing the inability of the catalyst to get the reactant inside. Mixed - behaviour was observed for intermediate parameter values, which we obtained in accordance with the theoretical results re-confirms the efficiency of the numerical methods used also.
One of the major upholding of using the Euler implicit methods, i.e, the global blanket of stability was exploited in this experience as we could choose the time and radius steps of our choice. The matrix obtained that had to be solved was a tri-diagonal matrix, which coukd be solved using Thomas algorithm with the most efficiency. So our overall scheme was computationally attractive for parametric studies and chemical engineering application.

6.3 Future Scope

For this paper, we had taken certain assumptions like Diffusivity value being constant and reaction rate happening inside the cat;yst being linear first order as we were more focussed in understanding the dependance of concentration profiles with these paramters, In the real world it might not be necessary that these values are remaining constant throughout the domain, they might be varying with time, concentration, etc. also. Some qualitative understanding for varying k and diffusivity values can be obtained from our results if we know in which direction are the k and De varying. But quantitativey determining the concentration profiles for varying Diffusivity and reaction coefficient will a future possibility of this paper.

7 Appendices

Parameter Definitions

Parameter	Symbol	Units	Description
Pellet radius	R	m	Radius of the spherical catalyst pellet
Radial position	r	m	Distance from the centre of the pellet ($0 \leq r \leq R$)
Reactant concentration	$C(r,t)$	$\mathrm{mol/m^3}$	Concentration of reactant at radial position r at time t
Bulk/surface concentration	C_s	$\mathrm{mol/m^3}$	Concentration of reactant at the pellet surface or in bulk fluid
Effective diffusivity	D_{eff}	$\mathrm{m^2/s}$	Diffusivity of the reactant inside porous pellet, accounting for porosity and tortuosity
Reaction rate	$R(C)$	$\mathrm{mol/(m^3{\cdot}s)}$	Rate of reaction per unit volume of pellet, function of local concentration
Reaction rate constant	k	$\mathrm{s^{-1}}$	Kinetic rate constant
Effectiveness factor	η	–	Ratio of actual reaction rate in the pellet to the rate if the entire pellet were at surface concentration
Concentration gradient	dC/dr	$\mathrm{mol/m^4}$	Rate of change of concentration with respect to radial position
Temperature	T	K	Temperature of the system
Pellet volume	V_p	$\mathrm{m^3}$	Total volume of the spherical pellet ($V_p = \frac{4}{3}\pi R^3$)
Surface area of pellet	A_s	$\mathrm{m^2}$	External surface area of the pellet ($A_s = 4\pi R^2$)
Thiele modulus	ϕ	–	Dimensionless number representing the ratio of reaction rate to diffusion rate inside the pellet: $\phi = R\sqrt{k/D_{\text{eff}}}$

References

[1] Rutherford Aris. *The Mathematical Theory of Diffusion and Reaction in Permeable Catalysts*. Oxford Engineering Science Series. Oxford: Oxford University Press, 1975.

[2] Bruce A. Finlayson. *Finite Difference Method for Reaction-Diffusion Problems*. Washington University Course Notes. Educational resource covering finite difference approximations for spatial and temporal derivatives in reaction-diffusion systems. Includes practical implementation details for solving parabolic PDEs in spherical coordinates using central difference schemes and discusses stability considerations. 2025. URL: https://faculty.washington.edu/finlayso/ebook/reaction/rxndiff/rxnFD.htm.

[3] H. Scott Fogler. *Elements of Chemical Reaction Engineering*. 5th. Prentice Hall, 2016. ISBN: 978-0134077100.

[4] W. Hao et al. "Stability and Robustness of Time-Discretization Schemes for Diffusion-Dominated Problems". In: *Journal of Computational Physics* TBD (2025). In press.

[5] A. N. F. Versypt. "Analysis of Finite Difference Discretization Schemes for Diffusion in Spherical Geometry with Variable Diffusivity". In: *International Journal of Numerical Methods for Heat & Fluid Flow* 24.7 (2014), pp. 1494–1510. DOI: 10.1108/HFF-07-2012-0157.

[6] Paul B. Weisz and Carroll D. Prater. "Interpretation of Measurements of Effective Diffusivity and Reaction Rate in a Catalyst Pellet". In: *Advances in Catalysis* 6 (1954), pp. 143–196.